Field-theory renormalization approach to the Kardar-Parisi-Zhang equation

Tao Sun and Michael Plischke
Department of Physics, Simon Fraser University, Burnaby, British Columbia, Canada V5A 1S6
(Received 27 December 1993)

The long wavelength scaling properties of the Kardar-Parisi-Zhang equation have been studied using a field-theory renormalization technique. The perturbation expansions are carried out to two-loop order for both $1+1$ and $2+1$ dimensions. In substrate dimension $d=1$, we find that the perturbation formalism obeys the fluctuation-dissipation theorem order by order so that the exact results $\chi=1/2$, $z=3/2$ are recovered in every order. For substrate dimension $d=2$, which is the critical dimension of this equation, an infrared stable strong coupling fixed point is found and the dynamic scaling exponents of this fixed point are obtained to be $\chi\simeq 0.16$, $z\simeq 1.84$, which are roughly halfway between the free field exponents and those determined by simulations of discrete models. The possible reasons for this discrepancy are discussed.

PACS number(s): 05.40.+j, 05.70.Ln, 64.60.Ht, 68.35.Fx

I. INTRODUCTION

The origin of the dynamic scaling properties and the identification of the universality classes in *far-from-equilibrium* growth processes have been extensively studied in the past decade. It has been found [1–13] that in a wide class of growth processes, such as ballistic deposition [8–10], the Eden growth process [6, 7, 11], and the restricted solid-on-solid (SOS) models [13], the height fluctuations in the interface behave as

$$\langle |h(\mathbf{x},t)-h(\mathbf{x}',t')|^2\rangle \sim |\mathbf{x}-\mathbf{x}'|^{2\chi}\, f\left(\frac{|t-t'|}{|\mathbf{x}-\mathbf{x}'|^{z}}\right) , \quad (1)$$

where $h(\mathbf{x},t)$ is the interface height variable at space-time point $(\mathbf{x},t)$, χ and z are respectively the roughening exponent and dynamic exponent for the interface, and the scaling function $f(x)$ has the well-known asymptotic behavior $f(x)\rightarrow$const as $x\rightarrow 0$ and $f(x)\sim x^{\chi/z}$ as $x\rightarrow\infty$.

It is generally believed that, for driven interface systems where growth is locally perpendicular to the existing surface, the growth process can be described by the Kardar-Parisi-Zhang (KPZ) equation [14, 15]

$$\frac{\partial h}{\partial t}=\nu\nabla^2 h+\tfrac{1}{2}\lambda\,(\nabla h)^2\,+\eta(\mathbf{x},t)\ , \quad (2)$$

where λ characterizes the lateral growth velocity, ν is an effective surface tension, and the noise $\eta(\mathbf{x},t)$ mimics the fluctuation in the deposition rate and satisfies the Gaussian distribution $\langle\eta(\mathbf{x},t)\rangle=0$, and

$$\langle\eta(\mathbf{x},t)\eta(\mathbf{x}',t')\rangle=2D\delta^d(\mathbf{x}-\mathbf{x}')\delta(t-t'). \quad (3)$$

Indeed, Eq. (2) provides a quantitive understanding of the fascinating morphology generated in a broad range of nonequilibrium processes [1–5]. Moreover, the understanding of the long wavelength scaling properties of Eq. (2) goes far beyond the interest of interface physics itself; it is of relevance to many applied fields, including the long-time behavior of randomly stirred fluids, directed polymers in random media, the evolution of Sivashinski flame fronts, and so on. A plausible explanation for this wide range of applications is that the KPZ equation is the simplest generalization of the diffusion equation that contains relevant nonlinearities [14, 15].

The widespread applicability of the KPZ equation and the technical importance of the processes being modeled have prompted much analytical [16–22, 28–30] and numerical [23–27] work on the KPZ equation. In fact, Eq. (2) can be mapped to the Burgers equation describing the fluid flow velocity in the presence of a random force by a transformation $\mathbf{v}=-\nabla h$ [14, 15]. Forster, Nelson, and Stephen (FNS) first studied this stochastic version of the Burgers equation by dynamic renormalization group techniques [16]. KPZ argued that the FNS results can be directly taken over to get the dynamic scaling form and the dynamic scaling exponents of Eq. (2) for $1+1$ dimensions [14]. According to these theories, the KPZ equation (2) satisfies a Galilean invariance, leading to a scaling relation

$$\chi+z=2, \quad (4)$$

for all dimensions. In $1+1$ dimensions, a fluctuation-dissipation theorem also holds, which allows one to calculate the exponents $\chi=\frac{1}{2}$, $z=\frac{3}{2}$ exactly. The $2+1$ dimension is the critical dimension of Eq. (2), at which only an unstable Gaussian fixed point is found in the one-loop approximation and the scaling exponents are therefore not obtained at this level of approximation.

Due to its practical importance, the subject of scaling properties of the KPZ equation in $2+1$ dimensions has aroused a tremendous amount of interest in the condensed matter physics community. Indeed, shortly after the KPZ theory was established, a number of groups employed direct numerical solution of Eq. (2) to get information about the values of the dynamic scaling exponent. However, their results are not in agreement with each other. The first two groups, Chakrabarti and Toral (CT) [23], and Guo, Grossmann, and Grant (GGG) [24, 25] found that $\chi\simeq 0.18\sim 0.24$, while later two other groups, Amar and Family (AF) [26], and Moser, Kertész,

1063-651X/94/49(6)/5046(12)/$06.00

and Wolf (MKW) [27] found that $\chi \simeq 0.39$, close to the conjecture of Kim and Kosterlitz based on numerical simulations of restricted SOS models [13]. To obtain the dynamic scaling exponents analytically, some approximation methods have also been proposed recently [28–30]. According to these studies, the roughening exponent in $2+1$ dimensions is in the range of $\chi \simeq 0.29-0.33$, which is close to the earlier numerical solutions presented by CT and GGG.

Although these studies do not agree well with one another in predicting the values of the dynamic scaling exponents, they do have one point in common: There exists a stable strong coupling fixed point governing the rough phase of the interface growth. Obviously, to obtain this strong coupling fixed point, a natural procedure is to extend the perturbation theory to higher order, i.e., a two-loop calculation in the renormalization group analysis. We have undertaken a systematic treatment of this model by means of the field-theoretic renormalization group. The perturbation expansion of the response function and the two-point correlation function have been performed to two-loop order in order to obtain the strong coupling fixed point in the critical dimension. In $1+1$ dimensions, the existence of the fluctuation-dissipation theorem is verified for every order in the perturbation expansion so that the exact results can be recovered within each order of approximation. For the $(2+1)$ dimensional case, we apply a *minimal-renormalization* [31–33] procedure to calculate the Wilson function and exponents. We find that, to the present order of approximation, $\chi \simeq 0.16$ and $z \simeq 1.84$. The purpose of this paper is to report on these calculations in some detail.

This paper is organized as follows. In Sec. II we illustrate the perturbation expansion of relevant vertex functions for both $1+1$ and $2+1$ dimensions. In Sec. III, we develop the renormalization group program to obtain the Wilson function and the dynamical scaling exponents. The strong coupling fixed point is exhibited and its infrared stability is discussed. Finally, our conclusions and some discussion of the results are given in Sec. IV.

II. PERTURBATION EXPANSION OF VERTEX FUNCTIONS

A. Martin-Siggia-Rose Lagrangian

Using the formalism developed by De Dominicis and Peliti [33], one can obtain a Martin-Siggia-Rose (MSR) [34] generating functional corresponding to the KPZ equation (2)

$$\mathcal{Z}\{l,\tilde{l}\} = \int \mathcal{D}\{h,i\tilde{h}\} \exp\left\{ \int_{k\omega} [\, h(k,\omega)l(-k,-\omega) + \tilde{h}(k,\omega)\tilde{l}(-k,-\omega)] + \mathcal{A}\{h,\tilde{h}\} \right\}, \tag{5}$$

where $\tilde{h}$ is the conjugate field of h, l and $\tilde{l}$ are sources, and the MSR action $\mathcal{A}\{h,\tilde{h}\}$ is given by

$$\mathcal{A}\{h,\tilde{h}\} = \int_{k,\omega} [-(-i\omega+\nu k^2)h(k,\omega)\tilde{h}(-k,-\omega) + D\tilde{h}(k,\omega)\tilde{h}(-k,-\omega)] + \left(-\frac{\lambda}{1!2!}\right) \int_{k\omega,q\Omega} [q\cdot(k-q)]\tilde{h}(-k,-\omega)h(q,\Omega)h(k-q,\omega-\Omega) \; . \tag{6}$$

Here k and q stand for the d-dimensional wave vectors and we have adopted a standard convention by defining

$$\int_{k\omega} \equiv \int_0^{\Lambda} \frac{d^dk}{(2\pi)^d} \int_{-\infty}^{\infty} \frac{d\omega}{2\pi} \; . \tag{7}$$

From the generating functional (5) one can generate exactly the same correlation functions and other quantities as those directly computed from Eq. (2).

In the MSR formalism, it is convenient to define generalized correlation functions of h and $\tilde{h}$, which can be written as

$$G_{N\tilde{N}}(\{k,\omega\}_N,\{k',\omega'\}_{\tilde{N}}) \equiv \langle h(k_1,\omega_1)...h(k_N,\omega_N)\tilde{h}(k_1',\omega_1')\ldots\tilde{h}(k_{\tilde{N}}',\omega_{\tilde{N}}')\rangle \; , \tag{8}$$

where $\{k,\omega\}$ means $\{k_1,\omega_1;...;k_N,\omega_N\}$ and the angular bracket means the average taken with the weight $\mathcal{Z}^{-1}\{0\}\exp\mathcal{A}$. In effect, $G_{N\tilde{N}}$ can be obtained from the generating functional (5) by taking derivatives with respect to the sources l and $\tilde{l}$. Namely,

$$G_{N\tilde{N}}(\{k,\omega\}_N,\{k',\omega'\}_{\tilde{N}}) = (2\pi)^{d(N+\tilde{N})}\, \mathcal{Z}^{-1}\{0\} \times \frac{\delta^{(N+\tilde{N})}}{\delta l_1\cdots\delta l_N \delta\tilde{l}_1\cdots\delta\tilde{l}_{\tilde{N}}} \times \mathcal{Z}\{l,\tilde{l}\}|_{l=\tilde{l}=0} \; , \tag{9}$$

where l_1 stands for $l(k_1,\omega_1)$, and so on. Note that the two functions G_{11} and G_{20} are identified as the usual response function and the usual two-point correlation function, respectively.

Since the standard renormalization procedures take the one-particle irreducible (1PI) vertex function $\Gamma_{N\tilde{N}}$, not the $G_{N\tilde{N}}$ functions, as basic functions, it is convenient to introduce the generating functional of $\Gamma_{N\tilde{N}}$ through a Legendre transformation

$$\Gamma\{\langle h\rangle,\langle\tilde{h}\rangle\} = -\ln\mathcal{Z}\{l,\tilde{l}\} + \int_{k,\omega} [\langle h(k,\omega)\rangle l(-k,-\omega) + \langle\tilde{h}(k,\omega)\rangle\tilde{l}(-k,-\omega)] \; , \tag{10}$$

where l and $\tilde{l}$ are considered as functionals of $\langle h\rangle$ and $\langle\tilde{h}\rangle$ satisfying the following equations:

$$\langle h \rangle = \frac{\delta \ln \mathcal{Z}}{\delta l} \ , \ \langle \tilde{h} \rangle = \frac{\delta \ln \mathcal{Z}}{\delta \tilde{l}} \ . \tag{11}$$

The vertex functions are then given by

$$\Gamma_{N\tilde{N}}(\{k,\omega\}_N, \{k',\omega'\}_{\tilde{N}}) = \prod_{i=1}^{N} \frac{\delta}{\delta \langle h(k_i,\omega_i)\rangle} \times \prod_{j=1}^{\tilde{N}} \frac{\delta}{\delta \langle \tilde{h}(k'_j,\omega'_j)\rangle} \times \Gamma\{\langle h\rangle, \langle \tilde{h}\rangle\}|_{\langle h\rangle = \langle \tilde{h}\rangle = 0} \ . \tag{12}$$

In fact, as we shall see below, it is sufficient to calculate three vertex functions Γ_{11}, Γ_{02}, and Γ_{21} to study the scaling behavior of the KPZ equation. At zero-loop order, we have

$$\Gamma_{11}^{(0)} = -i\omega + \nu k^2 \ , \ \Gamma_{02}^{(0)} = -2D \ ,$$
$$\Gamma_{21}^{(0)} = \frac{\lambda}{2} \ [q \cdot (k-q)] \ , \tag{13}$$

from which a classical version of the action (6) is recovered. Beyond the tree approximation, ultraviolet divergences appear when the cutoff $\Lambda \to \infty$ for $d \geq 2$. Equivalently, ultraviolet divergences will appear as poles at $\epsilon = 0$ when the theory is dimensionally regularized in $d = 2 - \epsilon$ dimensions.

B. Graph representation of vertex functions

We now proceed to discuss the perturbation expansion of the vertex functions Γ_{11}, Γ_{02}, and Γ_{21} in number of loops. Setting $\lambda = 0$, the free part of the generating functional (5) can be obtained exactly after carrying out the Gaussian integrals

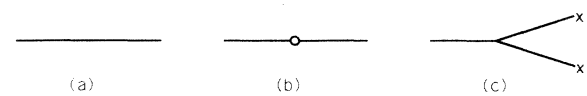

FIG. 1. Zero-order graphic representations of the response function (a), the correlation function (b), and the vertex function (c).

$$\mathcal{Z}^{(0)}\{l,\tilde{l}\} = \exp\left\{ \int_{k\omega} [G_{11}^{(0)}(k,\omega)\tilde{l}(k,\omega)l(-k,-\omega) + \tfrac{1}{2} G_{20}^{(0)}(k,\omega) l(k,\omega) l(-k,-\omega)] \right\}, \tag{14}$$

where $G_{11}^{(0)}$ and $G_{21}^{(0)}$ are given by

$$G_{11}^{(0)}(k,\omega) = [\ -i\omega \ + \ \nu k^2 \ ]^{-1} \ , \tag{15}$$

$$G_{20}^{(0)}(k,\omega) = 2D[(-i\omega + \nu k^2)(i\omega + \nu k^2)]^{-1}. \tag{16}$$

Thus, only two of the G functions defined in (8), i.e., G_{11} and G_{20}, have zero-order terms. In the language of Feynman graphs, $G_{11}^{(0)}$ and $G_{02}^{(0)}$ are called *propagator line* and *correlation line*, respectively. These are schematically shown in Figs. 1(a) and 1(b).

For the case of nonzero λ, making use of Eq. (14), the generating functional $\mathcal{Z}$ can be conveniently expressed as

$$\mathcal{Z}\{l,\tilde{l}\} = \exp\left((2\pi)^{3(d+1)} \ \mathcal{A}_{nl}\left\{ \frac{\delta}{\delta l}, \frac{\delta}{\delta \tilde{l}} \right\} \right) \mathcal{Z}^{(0)}\{l,\tilde{l}\} \ , \tag{17}$$

where the interacting action operator

$$\mathcal{A}_{nl}\left\{ \frac{\delta}{\delta l}, \frac{\delta}{\delta \tilde{l}} \right\} = -\frac{\lambda}{1!2!} \int_{k\omega q\Omega} [q \cdot (k-q)] \frac{\delta^3}{\delta \tilde{l}(k\omega) \delta l(-k+q, -\omega+\Omega) \delta l(-q,-\Omega)} \ . \tag{18}$$

Schematically, it is expressed in Fig. 1 (c). Note that the line without a cross is pointing in and the other two lines with a cross are pointing out. The momentum conservation law holds at the vertex. With these expressions, we are ready to discuss the perturbation expansion of vertex functions by means of graph representations.

Let us begin with Γ_{11}. From Eqs. (10) and (11), it is easy to show that $\Gamma_{11} = G_{11}^{-1}$. That is, the graphs of Γ_{11} can be obtained by drawing all 1PI graphs of G_{11} and omitting the external lines. Applying standard graphical techniques [31], the rules for constructing n-loop graphs of Γ_{11} can be summarized as follows:

(a) Draw $2n$ vertices without any connections.

(b) Choose one pointing-in line in one vertex and one pointing-out line (with cross) in the remaining vertices.

(c) Join all remaining end points with a cross in pairs to form the correlation lines (with a circle); join all lines with a cross to those without a cross in pairs to form propagator lines.

Note that there is in general more than one way to join the lines. Each way gives a separate term and all of them must be accounted for. Using the rules (a)–(c), one can construct all Feynman graphs of Γ_{11} easily. As shown in Fig. 2, there are one one-loop graph and 11 two-loop graphs for the vertex function Γ_{11}.

Next, we discuss graph representations of Γ_{02}. Similarly to Γ_{11}, the diagrammatic representation of Γ_{02} can be obtained by drawing all 1PI graphs of G_{20} without external lines. Therefore, the rules constructing the response function can be taken over with the following change in (b).

(b′) Choose two pointing-in lines among the vertices. In this way, as shown in Fig. 3, we have one one-loop graph and six two-loop graphs for the vertex function Γ_{02}.

Finally, because of the existence of Galilean invariance, the vertex function Γ_{21} remains tree-order unchanged. Therefore, we take advantage of this and do not perform the perturbation expansion of Γ_{21}. In fact, the two-loop order calculation of Γ_{21} seems to be barely feasible.

Next we summarize the rules that convert the graphs into algebraic expressions. From Eqs. (15), (16), (17), and (18), it is easy to determine the following rules:

(d) Label each line with a wave vector and frequency. The wave vectors and frequencies must obey conservation laws at each vertex, i.e., the incoming one must equal the sum of the outgoing two.

(e) Write a factor $[1/(2n)!]$ for an n-order graph. Write a factor $G_{11}^{(0)}$ for each propagator line and a factor $G_{20}^{(0)}$ for a correlation line. The values of k and ω are given for each line by the labels. Write $(-\frac{1}{1!2!}\lambda[q\cdot(k-q)])$ for each vertex, k and q being respectively the wave vector for the incoming line and one of those for the outgoing lines.

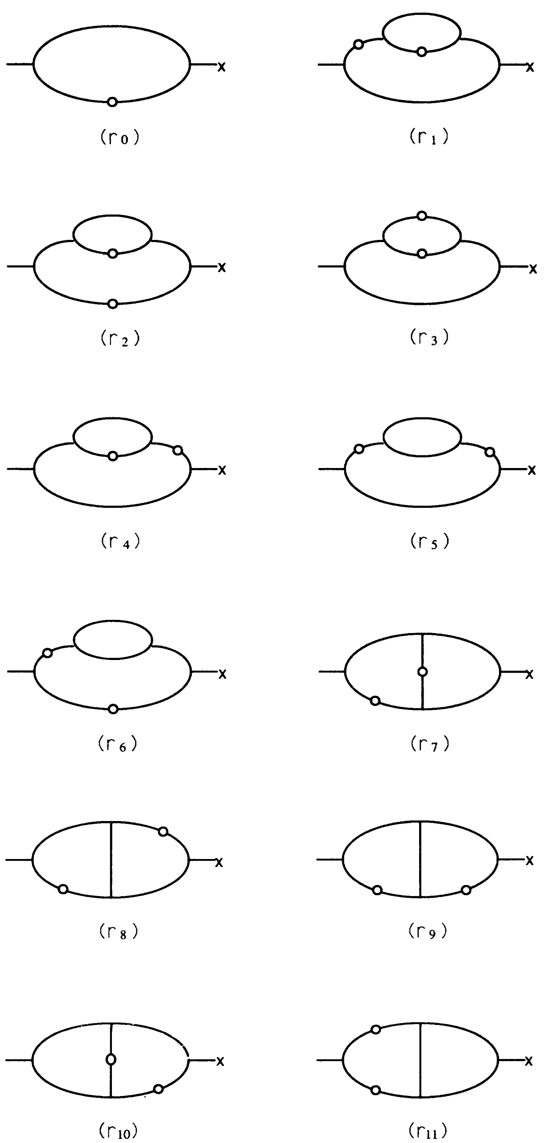

FIG. 2. One-loop and two-loop Feynman graphs of the response function. The corresponding symmetry factors are 4 for r_0, 8 for r_3, and 16 for all the remaining graphs.

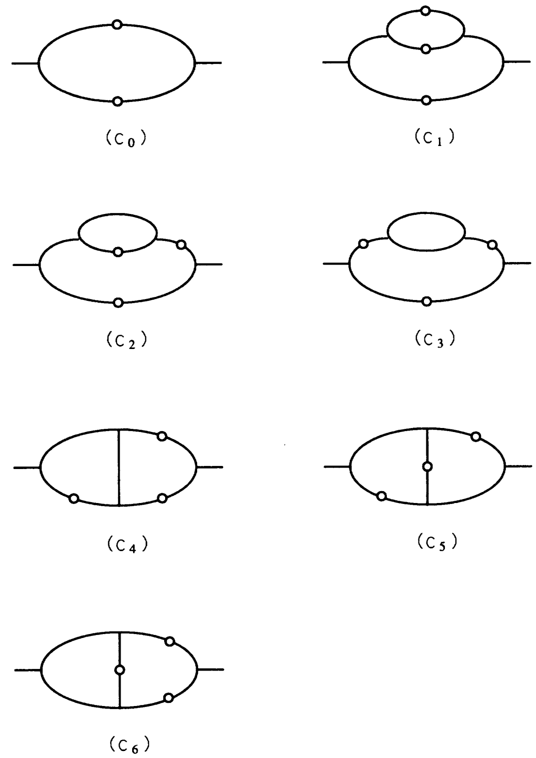

FIG. 3. One-loop and two-loop Feynman graphs of the two-point correlation function. The corresponding symmetry factors are 2 for c_0, 8 for c_1, 32 for c_2 and c_4, and 16 for c_5 and c_6.

(f) Integrate over all wave vectors and frequencies which are not fixed by the conservation laws mentioned in (d). A factor $(2\pi)^{-d-1}$ goes with each wave-vector–frequency integral.

The rules (a)–(f) form a complete set of rules for constructing graphs and writing down their contributions to the vertex functions Γ_{11} and Γ_{02}. The integrals over frequency are easy to carry out by means of the method of residues. All expressions of the Feynman graphs after performing the frequency integrals are listed in Appendix A and Appendix B. Next we discuss the calculation of the momentum integrals.

C. Calculation of vertex functions: $d=1$

It is well known that, in $d = 1$, the fluctuation-dissipation theorem holds for the KPZ equation [16]. Together with the Galilean invariance, the dynamic scaling exponents can be obtained exactly, i.e., $\chi = 1/2$, $z = 3/2$, independent of the order of the perturbation expansion. In this sense, the perturbation expansion and renormalization group program are superfluous for the case of $d = 1$, and any further discussion is unnecessary. However, if the perturbation program is performed in this dimension, the fluctuation-dissipation theorem should hold order by order in the perturbation expansions. This fact can be used to check the Feynman graph system and the corresponding symmetry factors. In Appendix C, we show that the relation

$$2D\Gamma_{11}(k\omega) = -\nu k^2 \Gamma_{02}(k\omega) \tag{19}$$

holds order by order. Therefore, we conclude that (i) the Feynman graph system developed in Sec. II B is consistent with the fluctuation-dissipation theorem in $d = 1$; (ii) the exact results $\chi = 1/2$ and $z = 3/2$ for this dimension can be recovered at both one- and two-loop order approximations.

D. Calculation of vertex functions: $d = 2$

In the higher dimensional case, the calculations become much more complicated. In particular, for the two-loop order terms, the two-variable integrals over momentum make the algebra itself quite tedious. However, since the minimal-renormalization procedure [31–33] only concerns the terms with poles in ϵ, one can ignore the finite part of the integrals and the calculation is substantially simplified.

First we consider $\Gamma_{11}(k,\omega)$. The one-loop graph is easy to calculate. As shown in Appendix A, it turns out that the divergent terms cancel each other so that there is no contribution to the renormalization group program from this order. For the 11 two-loop graphs, after the integrals over frequencies are performed, one has only 8 nonzero graphs to be computed. In Appendix A, we list all final results for the graphs in terms of the reduced coupling constant defined by

$$\bar{\lambda} \equiv \frac{\lambda D^{1/2}}{\nu^{3/2}} , \tag{20}$$

the external momentum k, and the external frequency ω. Summing up all contributions to the vertex function Γ_{11} to $O(1/\epsilon)$, we finally have

$$\Gamma_{11}(k,\omega) = -i\omega \left[1 + \frac{A_1}{\epsilon} K_d^2 \bar{\lambda}^4 k^{-2\epsilon} \right] + \nu k^2 \left[1 + \frac{A_2}{\epsilon} K_d^2 \bar{\lambda}^4 k^{-2\epsilon} \right] , \tag{21}$$

where the factor $K_d = 2\pi^{d/2}/[\Gamma(d/2)(2\pi)^d]$ is introduced for convenience and the two coefficients are given by

$$A_1 = -\tfrac{1}{16} + \tfrac{1}{16}\ln 2, \tag{22}$$

$$A_2 = \tfrac{1}{16}\ln 2. \tag{23}$$

Note that the leading term here is $O(1/\epsilon)$ rather than $O(1/\epsilon^2)$.

Now we turn to calculation of Γ_{02}. The calculation is similar to that of Γ_{11} but with three main differences. First, the external frequency ω can be set to zero, which makes the calculation easier. Next, there is a contribution from the one-loop graph. Finally, the leading term is $O(1/\epsilon^2)$, as expected. From the results listed in Appendix B and Eq. (13), we have the vertex function Γ_{02} to $O(1/\epsilon)$,

$$\Gamma_{02}(k,\omega) = -2D \left[1 + \frac{B_1}{\epsilon} K_d \bar{\lambda}^2 k^{-\epsilon} + \frac{B_2}{\epsilon^2} K_d^2 \bar{\lambda}^4 k^{-2\epsilon} \right] , \tag{24}$$

where the two coefficients are given by

$$B_1 = \tfrac{1}{4} , \quad B_2 = \tfrac{1}{16} . \tag{25}$$

Note that $B_1^2 = B_2$ which ensures that the so called *magic* cancellation occurs. In effect, this is one of the intrinsic features of the field-theoretic renormalization program, following directly from the fact that the KPZ theory is renormalizable at its critical dimension [31]. This point will be discussed further in the next section.

Finally, we discuss the vertex function Γ_{21}. As mentioned in Sec. II B, since the KPZ equation (2) is invariant under Galilean transformation, the vertex function Γ_{21} will remain unchanged from its zero order, i.e.,

$$\Gamma_{21}(k,\omega;q,\Omega) = \frac{\lambda}{2} [q \cdot (k-q)] . \tag{26}$$

This concludes the calculation of the vertex functions Γ_{11}, Γ_{02}, and Γ_{21} up to two-loop order. All terms beyond the tree approximation in the expressions involve poles in ϵ. To remove these divergences and obtain the dynamic scaling properties of the KPZ equation, one has to apply the renormalization group theory. This is the content of the next section.

III. RENORMALIZATION GROUP AND SCALING PROPERTIES

A. Dimensional analysis

We briefly list here the canonical dimensions of various quantities in the theory. These will be used in the discussion of the scaling behavior of the vertex functions. The dimension of the quantities can be determined by requiring that $[\mathcal{A}] = 0$ and expressing the dimensionality in wave-vector units.

(i) Coefficients, frequency, and the reduced coupling constant.

$$[\nu] = d_\nu , [D] = d_D$$

$$[\lambda] = d_\lambda = \frac{\epsilon}{2} + \frac{3}{2} d_\nu - \frac{1}{2} d_D , \tag{27}$$

$$[\omega] = 2 + d_\nu , \quad [\bar{\lambda}] = \frac{\epsilon}{2} . \tag{28}$$

(ii) Height fields in Fourier space.

$$[h(k,\omega)] = -\frac{6+d}{2} - \frac{3}{2} d_\nu + \frac{1}{2} d_D , \tag{29}$$

$$[\tilde{h}(k,\omega)] = -\frac{2+d}{2} - \frac{1}{2} d_\nu - \frac{1}{2} d_D . \tag{30}$$

(iii) Vertex functions in Fourier space. In view of Eqs. (12), (29), and (30), after the overall momentum conserving δ function is removed, we have

$$[\Gamma_{N\tilde{N}}] \equiv d_{N\tilde{N}}, \tag{31}$$

where

$$d_{N\tilde{N}} = d+2+\frac{2-d}{2}N - \frac{2+d}{2}\tilde{N} + \frac{N-\tilde{N}+2}{2}\, d_\nu - \frac{N-\tilde{N}}{2}\, d_D \; . \tag{32}$$

In particular,

$$d_{11} = 2 + d_\nu \; , \; d_{02} = d_D \; . \tag{33}$$

The canonical dimensions of ν and D, i.e., the values of d_ν and d_D, cannot be determined by the theory. As we shall see later, the final dynamic scaling properties do not depend on their exact values. However, they are relevant for the derivation of the dynamic scaling form.

B. Renormalization of vertex functions

To remove the divergences that appear in the perturbation expansions of the vertex functions, we introduce five renormalization functions, which are listed below.

(i) Height-field renormalization.

$$h = Z^{1/2}\, h^r \; , \; \tilde{h} = \tilde{Z}^{1/2}\, \tilde{h}^r \; . \tag{34}$$

(ii) Coefficient renormalization.

$$\sigma = Z_\sigma^{-1}\, \sigma^r \; , \; \sigma = \nu, D, \lambda \; . \tag{35}$$

(iii) Reduced coupling constant. It is convenient to introduce two dimensionless constants

$$K_d^{1/2}\bar{\lambda} \equiv u_0\kappa^{\epsilon/2} \; , \; K_d^{1/2}\bar{\lambda}^r \equiv u\kappa^{\epsilon/2} \; , \tag{36}$$

where κ is a reference wave number. Using the three renormalization functions $\{Z_\sigma\}$ introduced above, the coupling constant can be renormalized as, from Eqs. (20) and (35),

$$u_0^2 = \frac{Z_\nu^3}{Z_\lambda^2 Z_D}\, u^2 \; . \tag{37}$$

(iv) Vertex functions. Similar to the coupling constant, the vertex functions can also be renormalized without introducing new Z functions,

$$\Gamma^r_{N\tilde{N}}(\{k,\omega\};\{\sigma^r\},u;\kappa) = Z^{N/2}\, \tilde{Z}^{\tilde{N}/2}\, \Gamma_{N\tilde{N}}(\{k,\omega\};\{\sigma\},u_0;\Lambda) \; , \tag{38}$$

where $\sigma = \nu, D, \lambda$. In particular,

$$\Gamma^r_{11}(k,\omega;\{\sigma^r\},u;\kappa) = (Z\tilde{Z})^{1/2}\Gamma_{11}(k,\omega;\{\sigma\},u_0;\Lambda) \; , \tag{39}$$

$$\Gamma^r_{02}(k,\omega;\{\sigma^r\},u;\kappa) = \tilde{Z}\Gamma_{02}(k,\omega;\{\sigma\},u_0;\Lambda) \; , \tag{40}$$

$$\Gamma^r_{21}(\{k,\omega\};\{\sigma^r\},u;\kappa) = Z\tilde{Z}^{1/2}\Gamma_{21}(\{k,\omega\};\{\sigma\},u_0;\Lambda) \; . \tag{41}$$

We now have five renormalization functions, namely Z, $\tilde{Z}$, and Z_σ ($\sigma = \nu, D, \lambda$), to be determined by the conditions given in Eqs. (37)–(41).

C. Callan-Symanzik equations and Wilson function

The renormalization program discussed above assures that a finite theory can be obtained by introducing the renormalization functions. That is, the divergences appearing in the perturbation expansion series can be removed by redefining the height fields and the coefficients. Nevertheless, the most important usage of the renormalization program lies in the fact that it leads to a very beautiful formalism, i.e., the renormalization group theory, which enables us to study the scaling behavior of the system. We begin with the derivation of the renormalization group equation of the KPZ model. Consider first Eq. (38). Since the bare vertex function in the right-hand side of Eq. (38) is independent of the reference wave number κ, we have

$$\left(\kappa\frac{\partial}{\partial\kappa}\right)_0 [Z^{-N/2}\tilde{Z}^{-\tilde{N}/2}\, \Gamma^r_{N\tilde{N}}(\{k,\omega\};\{\sigma^r\},u;\kappa)] = 0 \; , \tag{42}$$

where $(\kappa\partial/\partial\kappa)_0$ means that the derivatives are taken at fixed bare parameters. After performing the derivatives, Eq. (42) can be rewritten as

$$\left[\kappa\frac{\partial}{\partial\kappa} + \beta(u)\frac{\partial}{\partial u} + \sum_\sigma \zeta_\sigma\sigma^r\frac{\partial}{\partial\sigma^r} - \frac{N}{2}\gamma - \frac{\tilde{N}}{2}\tilde{\gamma}\right] \times\Gamma^r_{N\tilde{N}}(\{k,\omega\};\{\sigma^r\},u;\kappa) = 0 \; , \tag{43}$$

where the Wilson function

$$\beta(u) = \left(\kappa\frac{\partial u}{\partial\kappa}\right)_0 \; , \tag{44}$$

and the five exponents are given by

$$\zeta_\sigma = \kappa\left(\frac{\partial\ln Z_\sigma}{\partial\kappa}\right)_0 \; , \; \sigma = \nu, D, \lambda \; , \tag{45}$$

$$\gamma = \kappa\left(\frac{\partial\ln Z}{\partial\kappa}\right)_0 \; , \tag{46}$$

$$\tilde{\gamma} = \kappa\left(\frac{\partial\ln\tilde{Z}}{\partial\kappa}\right)_0 \; . \tag{47}$$

Equation (43) is the Callan-Symanzik equation, or sometimes called the renormalization group equation, of the KPZ model. Note that the Wilson function $\beta(u)$ and all exponents are finite when $\Lambda\to\infty$ at $d = 2$ due to the fact that $\Gamma^r_{N\tilde{N}}$ is finite in this limit. The Wilson function can be expressed in a convenient form

$$\beta(u) = -\frac{\epsilon}{2}\left(\frac{\partial\ln u_0}{\partial u}\right)^{-1} \; . \tag{48}$$

Similarly, for the exponents, we have

$$\zeta_\sigma = \beta(u)\frac{\partial\ln Z_\sigma}{\partial u} \; , \; \sigma = \nu, D, \lambda \; , \tag{49}$$

$$\gamma = \beta(u)\frac{\partial\ln Z}{\partial u} \; , \tag{50}$$

$$\tilde{\gamma} = \beta(u)\frac{\partial\ln\tilde{Z}}{\partial u} \; . \tag{51}$$

These expressions will be used in the calculation of the fixed point and its dynamic scaling exponents.

By means of the standard method of characteristics, the differential equation (43) can be solved and the vertex function $\Gamma^r_{N\tilde{N}}$ reads

$$\Gamma^r_{N\tilde{N}}(\{k,\omega\};\{\sigma^r(\rho)\},u(\rho);\kappa\rho)$$

$$= \exp\left\{\int_1^\rho \frac{dx}{x}\left[\frac{N}{2}\gamma(x)+\frac{\tilde{N}}{2}\tilde{\gamma}(x)\right]\right\} \times\Gamma^r_{N\tilde{N}}(\{k,\omega\};\{\sigma^r\},u;\kappa) \ , \tag{52}$$

where the characteristic equations are

$$\beta(u(\rho)) = \rho\frac{du(\rho)}{d\rho} \ , \tag{53}$$

$$\zeta_\sigma(u(\rho)) = \rho\frac{d\ln\sigma^r(\rho)}{d\rho} \ , \tag{54}$$

with the initial conditions $u(1) = u$ and $\sigma^r(1) = \sigma^r$. Since the vertex function $\Gamma_{N\tilde{N}}$ has dimension $d_{N\tilde{N}}$ given in Eq. (32), it is convenient to define a dimensionless function $\Phi_{N\tilde{N}}$ by [35]

$$\Gamma^r_{N\tilde{N}}(\{k,\omega\};\{\sigma^r\},u;\kappa) \equiv \kappa^{d_{N\tilde{N}}}\Phi_{N\tilde{N}}\left(\left\{\frac{k}{\kappa},\frac{\omega}{\kappa^{2+d_\nu}}\right\};\left\{\frac{\sigma^r}{\kappa^{d_\sigma}}\right\},u\right). \tag{55}$$

Therefore, by Eq. (52), it follows that

$$\Phi_{N\tilde{N}}\left(\left\{\frac{k}{\kappa},\frac{\omega}{\kappa^{2+d_\nu}}\right\};\left\{\frac{\sigma^r}{\kappa^{d_\sigma}}\right\},u\right) = \rho^{d_{N\tilde{N}}}\exp\left\{-\int_1^\rho \frac{dx}{x}\left[\frac{N}{2}\gamma(x)+\frac{\tilde{N}}{2}\tilde{\gamma}(x)\right]\right\} \times\Phi_{N\tilde{N}}\left(\left\{\frac{k}{\kappa\rho},\frac{\omega}{(\rho\kappa)^{2+d_\nu}}\right\};\left\{\frac{\sigma^r(\rho)}{(\rho\kappa)^{d_\sigma}}\right\},u(\rho)\right). \tag{56}$$

In order to obtain scaling relations, we assume that there exist fixed points at which the reduced coupling constant u reaches a value u^* such that any change in the scale of the momenta does not affect it. Therefore, from Eq. (53), the fixed points are determined by

$$\beta(u^*) = 0 \ . \tag{57}$$

The asymptotic form of the vertex function is given by the vertex function taken at the fixed point. Correspondingly, we have

$$\Phi^{\rm as}_{N\tilde{N}} = \Phi_{N\tilde{N}}\left(\left\{\frac{k}{\kappa},\frac{\omega}{\kappa^{2+d_\nu}}\right\};\left\{\frac{\sigma^r}{\kappa^{d_\sigma}}\right\},u^*\right) \ . \tag{58}$$

Making use of Eq. (56), we obtain

$$\Phi^{\rm as}_{N\tilde{N}} = \rho^{d_{N\tilde{N}}-\frac{1}{2}(N\gamma^*+\tilde{N}\tilde{\gamma}^*)} \times\Phi_{N\tilde{N}}\left(\left\{\frac{k}{\kappa\rho},\frac{\omega}{(\rho\kappa)^{2+d_\nu}}\right\};\left\{\frac{\sigma^r\rho^{\zeta^*_\sigma}}{(\rho\kappa)^{d_\sigma}}\right\},u^*\right) \ . \tag{59}$$

Setting

$$\rho = \frac{k}{\kappa} \ , \quad \frac{\nu^r\rho^{\zeta^*_\nu}}{(\rho\kappa)^{d_\nu}} = 1 \ , \quad \frac{D^r\rho^{\zeta^*_D}}{(\rho\kappa)^{d_D}} = 1 \ , \tag{60}$$

we have

$$\Phi^{\rm as}_{N\tilde{N}} = \left(\frac{k}{\kappa}\right)^{d_{N\tilde{N}}-\frac{1}{2}(N\gamma^*+\tilde{N}\tilde{\gamma}^*)} \times\Phi_{N\tilde{N}}\left(\left\{\frac{\omega}{\nu^r k^2(\frac{k}{\kappa})^{\zeta^*_\nu}}\right\};u^*\right) \ . \tag{61}$$

From Eq. (55), the asymptotic form of the vertex function is given by

$$\Gamma^{\rm as}_{N\tilde{N}} = k^{d_{N\tilde{N}}}\left(\frac{k}{\kappa}\right)^{-\frac{1}{2}(N\gamma^*+\tilde{N}\tilde{\gamma}^*)} \times\Phi_{N\tilde{N}}\left(\left\{\frac{\omega}{\nu^r k^2(\frac{k}{\kappa})^{\zeta^*_\nu}}\right\};u^*\right) \ . \tag{62}$$

In particular, we consider the cases of $N = \tilde{N} = 1$ and $N = 0$, $\tilde{N} = 2$. From Eq. (62), we have

$$\Gamma^{\rm as}_{11}(k,\omega) = k^{d_{11}}\left(\frac{k}{\kappa}\right)^{-\frac{1}{2}(\gamma^*+\tilde{\gamma}^*)}\Phi_{11}\left(\frac{\omega}{\nu^r k^2(\frac{k}{\kappa})^{\zeta^*_\nu}}\right) \ , \tag{63}$$

$$\Gamma^{\rm as}_{02}(k,\omega) = k^{d_{02}}\left(\frac{k}{\kappa}\right)^{-\tilde{\gamma}^*}\Phi_{02}\left(\frac{\omega}{\nu^r k^2(\frac{k}{\kappa})^{\zeta^*_\nu}}\right) \ . \tag{64}$$

A few algebraic manipulations yield the asymptotic form of the two-point correlation function,

$$G^{\rm as}_{20}(k,\omega) = k^{d_D-2d_\nu-4}\left(\frac{k}{\kappa}\right)^{\gamma^*}\Phi_{20}\left(\frac{\omega}{\nu^r k^2(\frac{k}{\kappa})^{\zeta^*_\nu}}\right) \ , \tag{65}$$

from which the dynamic scaling exponents can be identified as

$$z = 2 + \zeta^*_\nu \ , \quad \chi = -\tfrac{1}{2}(\gamma^* + \zeta^*_\nu) \ . \tag{66}$$

We shall devote the following part of this section to the calculation of these exponents.

D. Dynamic scaling exponents

According to the discussion presented in Sec. II B, there are six renormalization constants, Z, $\tilde{Z}$, $Z_\sigma(\sigma = \nu, D, \lambda)$, and u_0, to be calculated. These quantities are not universal in the sense that they remove all divergences from the perturbation expansion of the vertex functions. They depend on the particular normalization conditions one applies. But the universal quantities describing the physics of the system, such as the dynamic scaling exponents, are identical for all renormalization programs used. Here we apply the minimal-renormalization procedure [31–33] to determine the renormalization constants. That is, they are obtained by deciding that the renormalization constants just remove the poles in ϵ of the divergent vertex functions.

First of all, we express the renormalization constants formally in terms of power series in the variable u,

$$u_0 = u(1 + a_2u^2 + a_4u^4) \ , \tag{67}$$

$$Z_\sigma = 1 + b_{\sigma 2}u^2 + b_{\sigma 4}u^4 \ , \quad \sigma = \nu, D, \lambda \ , \tag{68}$$

$$Z = 1 + c_2u^2 + c_4u^4 \ , \tag{69}$$

$$\tilde{Z} = 1 + d_2u^2 + d_4u^4 \ . \tag{70}$$

Thus the task is to calculate the coefficients a_2, a_4, and so on by the requirement that poles in ϵ be minimally subtracted. Further inspections reveal that there are only five conditions available in our minimal-renormalization program, which can be found from Eqs. (37), (39), (40), and (41). This implies that the coefficients a_2-d_4 cannot be completely obtained. However, from Eqs. (48), (49), and (66), we see that to obtain the scaling exponents all we need to know are the quantities u_0 and Z_ν. After some simple algebraic manipulations, we find that these two renormalization constants can be determined uniquely, and can be written as

$$u_0 = u\left\{1 - \frac{B_1}{2\epsilon}\, u^2 + \left[\frac{A_1+3A_2}{2}\frac{1}{\epsilon} + \frac{7B_1^2-4B_2}{8}\frac{1}{\epsilon^2}\right] u^4\right\}, \tag{71}$$

$$Z_\nu = 1 + 0\times u^2 - (A_1 - A_2)\frac{1}{\epsilon}\, u^4 , \tag{72}$$

where the coefficients A_1, A_2, B_1, and B_2 are given in the previous section.

Substituting these expressions into Eqs. (48) and (49), one obtains the Wilson function $\beta(u)$ and the exponent $\zeta_\nu(u)$ as power series of u. To the order required, we have

$$\beta(u) = u\left[-\frac{\epsilon}{2} - \frac{B_1}{2}u^2 + \left(A_1 + 3A_2 + \frac{B_1^2 - B_2}{\epsilon}\right)u^4\right], \tag{73}$$

$$\zeta_\nu = 2\,(A_1 - A_2)\, u^4 . \tag{74}$$

Now let us consider Eq. (73). As mentioned before, the Wilson function $\beta(u)$ must be finite in the limit $\epsilon \to 0$. This requires that the coefficients of the terms with poles in ϵ must cancel each other. Namely, we must have $B_1^2 - B_2 = 0$. Equation (25) shows that this relation is satisfied, as mentioned in the previous section.

Now we are ready to calculate the fixed point and its dynamic scaling exponents. Setting the right-hand side of Eq. (73) to zero, the strong coupling fixed point for $d = 2$ is found to be

$$(u^2)^* = \frac{B_1}{2(A_1+3A_2)} = \frac{2}{4\ln 2 - 1} . \tag{75}$$

It is easy to show that $\frac{d\beta(u)}{du}\big|_{u^*} > 0$, so that this fixed point is infrared stable. Substituting the above expression into Eqs. (66) and (74), we obtain the dynamic exponent at this fixed point

$$z = 2 - \frac{1}{2(4\ln 2-1)^2} \simeq 1.84 , \tag{76}$$

which implies the roughening exponent

$$\chi \simeq 0.16 . \tag{77}$$

The value of χ is smaller than the values found from simulations of discrete models. In the next section, we shall comment on the difference.

IV. DISCUSSION AND CONCLUSION

We have studied the long wavelength properties of the Kardar-Parisi-Zhang equation using field-theoretic renormalization techniques. In substrate dimension $d = 1$, the perturbation expansion series of the response function and the two-point correlation function are found to obey the fluctuation-dissipation theorem order by order, indicating that the exact results $\chi = 1/2$, $z = 3/2$ can be obtained perturbatively to both one- and two-loop order approximations. In substrate dimension $d = 2$, a renormalization group program has been developed and a stable strong coupling fixed point has been found. This fixed point governs a rough state of the driven interface with the dynamic scaling exponents $\chi \simeq 0.16$, $z \simeq 1.84$.

Even though the relationship between the KPZ equation and the discrete models has not been rigorously established yet, it is generally believed that these models belong to the same universality class. However, the dynamic scaling exponents obtained in our study are clearly different from the results of numerical simulations on the discrete models. If we accept the universality conjecture, then the difference must arise from the perturbation expansion. Clearly, our fixed point value u^* cannot survive to the next order approximations and there is no measure telling us how close our u^* is to its true value. In fact, the renormalization group study in the critical dimension is problematical since the loop expansion is not an expansion in a small parameter and one does not have a small parameter to control the perturbation expansion ($\epsilon = 0$). This is a fundamental problem of the renormalization group theory [31]. Nevertheless, presently it is the only way one can systematically obtain the strong coupling fixed point of the KPZ equation in the critical dimension.

Two interesting features of this study are worth noting. First, the strong coupling fixed point (75) does not connect to the conventional strong coupling fixed point in $1 + 1$ dimensions [14–16]. Besides the strong coupling fixed point (75), there is another fixed point which is proportional to ϵ. This fixed point is unstable and becomes Gaussian in the critical dimension, and corresponds to the conventional strong coupling fixed point in $1 + 1$ dimensions. Unfortunately, one cannot obtain the $1+1$ dimension scaling properties from this fixed point by the traditional ϵ expansion formalism due to its unstable nature. Secondly, the functional renormalization group studies [19, 21] and the self-consistent approaches [28, 29] have raised the possibility of a finite upper critical dimensionality beyond which the strong coupling exponents become equal to those at weak coupling. Clearly, this property is not observed in our studies. We believe that this matter cannot be elucidated by the present calculation. In fact, we are strongly bound to the neighborhood of the critical dimensionality by the field-theoretic renormalization group method that we use [31].

In conclusion, we obtained the strong coupling fixed point of the KPZ equation for physically interesting dimensions. Our results $\chi \simeq 0.16$ and $z \simeq 1.84$ are consistent with the earlier numerical results of [23–25]. However, due to the reason stated above, we do not resolve the controversy between the results of Refs. [23–25] and [26, 27]. Our values of the dynamic scaling exponents result from the leading nontrivial approximation to the strong coupling fixed point. Presumably, these results could be modified by contributions from the next and higher order terms in perturbation theory.

ACKNOWLEDGMENTS

We thank M. Grant, J. M. Kosterlitz, and M. Kardar for many useful discussions. This work was supported by the Natural Sciences and Engineering Research Council of Canada.

APPENDIX A: INTEGRALS FOR RESPONSE FUNCTION

In this Appendix we list all expressions of Feynman graphs of the response function and their final results in $2-\epsilon$ dimensions to order $O(1/\epsilon)$.

1. One-loop order

$$r_0 = \nu\left(-\frac{\bar\lambda}{1!2!}\right)^2 \int_p \frac{[q\cdot(k-q)](k\cdot q)}{q^2[-i\omega/\nu + q^2 + (k-q)^2]}$$
$$= \nu\left(-\frac{\bar\lambda}{1!2!}\right)^2 \frac{k^{2-\epsilon}}{(4\pi)^{d/2}}\left[\frac{1}{\epsilon}\times 0 + O(1)\right].$$

2. Two-loop order

$$r_1 = \nu\left(-\frac{\bar\lambda}{1!2!}\right)^4 \int_{pq} \frac{[q\cdot(k-q)][p\cdot(q-p)](k\cdot q)(q\cdot p)}{2q^4p^2[-i\omega/\nu + q^2 + (k-q)^2][q^2+p^2+(q-p)^2]}$$
$$= \nu\left(-\frac{\bar\lambda}{1!2!}\right)^4 \frac{k^{2-2\epsilon}}{(4\pi)^d}\left[\frac{1}{\epsilon}\times 0 + O(1)\right],$$

$$r_2 = \nu\left(-\frac{\bar\lambda}{1!2!}\right)^4 \int_{pq} \frac{[q\cdot(k-q)][p\cdot(q-p)][k\cdot(k-q)](q\cdot p)}{p^2(k-q)^2[-i\omega/\nu + q^2 + (k-q)^2]^2}\,\frac{1}{-i\omega/\nu + p^2 + (k-q)^2 + (q-p)^2}$$
$$= \nu\left(-\frac{\bar\lambda}{1!2!}\right)^4 \frac{k^{2-2\epsilon}}{(4\pi)^d}\left[\frac{1}{\epsilon}\frac{1}{24} + O(1)\right],$$

$$r_3 = \nu\left(-\frac{\bar\lambda}{1!2!}\right)^4 \int_{pq} [q\cdot(k-q)][p\cdot(q-p)]^2(-k\cdot q)$$
$$\times \frac{-i\omega/\nu + q^2 + p^2 + (k-q)^2 + (q-p)^2}{q^2p^2(q-p)^2[-i\omega/\nu + q^2 + (k-q)^2][q^2+p^2+(q-p)^2]}\,\frac{1}{-i\omega/\nu + p^2 + (k-q)^2 + (q-p)^2}$$
$$= \nu\left(-\frac{\bar\lambda}{1!2!}\right)^4 \frac{k^{2-2\epsilon}}{(4\pi)^d}\left[\frac{1}{\epsilon}\left(\frac{7}{72} - \ln 2 + \frac{1}{4}\ln 3\right) + O(1)\right]$$
$$+ \left(-\frac{\bar\lambda}{1!2!}\right)^4 \frac{k^{-2\epsilon}}{(4\pi)^d}(-i\omega)\left[\frac{1}{\epsilon}\left(\frac{1}{2} - \frac{1}{2}\ln 2\right) + O(1)\right],$$

$$r_4 = \nu\left(-\frac{\bar\lambda}{1!2!}\right)^4 \int_{pq} [q\cdot(k-q)][p\cdot(q-p)](k\cdot q)(q\cdot p)$$
$$\times \frac{[q^2+(k-q)^2]^2 + [3q^2 + (k-q)^2][q^2+p^2+(q-p)^2]}{2q^4p^2[-i\omega/\nu + q^2 + (k-q)^2]^2[q^2+p^2+(q-p)^2]}\,\frac{1}{-i\omega/\nu + p^2 + (k-q)^2 + (q-p)^2}$$
$$= \nu\left(-\frac{\bar\lambda}{1!2!}\right)^4 \frac{k^{2-2\epsilon}}{(4\pi)^d}\left[\frac{1}{\epsilon}\left(-\frac{7}{144}\right) + O(1)\right],$$

$$r_7 = \nu\left(-\frac{\bar\lambda}{1!2!}\right)^4 \int_{pq} \frac{[q\cdot(k-q)][p\cdot(q-p)][(k-p)\cdot(q-p)](-k\cdot p)}{q^2(q-p)^2[-i\omega/\nu+q^2+(k-q)^2][q^2+p^2+(q-p)^2]}\,\frac{1}{-i\omega/\nu+q^2+(k-p)^2+(q-p)^2}$$
$$= \nu\left(-\frac{\bar\lambda}{1!2!}\right)^4 \frac{k^{2-2\epsilon}}{(4\pi)^d}\left[\frac{1}{\epsilon}\left(-\frac{7}{144}+\frac{3}{8}\ln 2-\frac{1}{8}\ln 3\right) + O(1)\right]$$
$$+\left(-\frac{\bar\lambda}{1!2!}\right)^4 \frac{k^{-2\epsilon}}{(4\pi)^d}(-i\omega)\left[\frac{1}{\epsilon}\left(-\frac{1}{8}+\frac{1}{8}\ln 2\right) + O(1)\right],$$

$$r_8 = \nu\left(-\frac{\bar\lambda}{1!2!}\right)^4 \int_{pq} \frac{[q\cdot(k-q)][p\cdot(q-p)][(k-q)\cdot(k-p)](k\cdot p)}{p^2(k-q)^2[-i\omega/\nu+q^2+(k-q)^2]}$$
$$\times\frac{1}{[-i\omega/\nu+p^2+(k-p)^2][-i\omega/\nu+p^2+(k-q)^2+(q-p)^2]}$$
$$= \nu\left(-\frac{\bar\lambda}{1!2!}\right)^4 \frac{k^{2-2\epsilon}}{(4\pi)^d}\left[\frac{1}{\epsilon}\left(-\frac{1}{48}+\frac{1}{8}\ln 3\right) + O(1)\right]$$
$$+\left(-\frac{\bar\lambda}{1!2!}\right)^4 \frac{k^{-2\epsilon}}{(4\pi)^d}(-i\omega)\left[\frac{1}{\epsilon}\left(-\frac{1}{4}+\frac{1}{4}\ln 2\right) + O(1)\right],$$

$$r_9 = \nu\left(-\frac{\bar\lambda}{1!2!}\right)^4 \int_{pq}[q\cdot(k-q)][(k-p)\cdot(q-p)](-k\cdot p)$$
$$\times\frac{-i\omega/\nu+q^2+p^2+(k-p)^2+(q-p)^2}{q^2p^2(q-p)^2[-i\omega/\nu+q^2+(k-q)^2][q^2+p^2+(q-p)^2]}$$
$$\times\frac{1}{[-i\omega/\nu+p^2+(k-p)^2][-i\omega/\nu+q^2+(k-p)^2+(q-p)^2]}$$
$$= \nu\left(-\frac{\bar\lambda}{1!2!}\right)^4 \frac{k^{2-2\epsilon}}{(4\pi)^d}\left[\frac{1}{\epsilon}\left(\frac{1}{72}-\frac{1}{8}\ln 2\right) + O(1)\right]$$
$$+\left(-\frac{\bar\lambda}{1!2!}\right)^4 \frac{k^{-2\epsilon}}{(4\pi)^d}(-i\omega)\left[\frac{1}{\epsilon}\left(\frac{1}{8}-\frac{1}{8}\ln 2\right) + O(1)\right],$$

$$r_{10} = \nu\left(-\frac{\bar\lambda}{1!2!}\right)^4 \int_{pq}[q\cdot(k-q)][p\cdot(q-p)][(k-p)\cdot(q-p)](k\cdot p)$$
$$\times\left\{\frac{[-2i\omega/\nu+q^2+p^2+(k-q)^2+(k-p)^2+2(q-p)^2]}{p^2(q-p)^2[-i\omega/\nu+q^2+(k-q)^2][q^2+p^2+(q-p)^2]}\right.$$
$$\times\frac{[q^2+p^2+(q-p)^2]}{[-i\omega/\nu+q^2+(k-p)^2+(q-p)^2][-i\omega/\nu+p^2+(k-q)^2+(q-p)^2]}$$
$$\times\frac{1}{-i\omega/\nu+p^2+(k-p)^2}+\frac{[-i\omega/\nu+p^2+(k-p)^2]}{p^2(q-p)^2[-i\omega/\nu+q^2+(k-q)^2][q^2+p^2+(q-p)^2]}$$
$$\left.\times\frac{[-i\omega/\nu+p^2+(k-q)^2+(q-p)^2]}{[-i\omega/\nu+q^2+(k-p)^2+(q-p)^2][-i\omega/\nu+p^2+(k-q)^2+(q-p)^2]}\,\frac{1}{-i\omega/\nu+p^2+(k-p)^2}\right\}$$
$$= \nu\left(-\frac{\bar\lambda}{1!2!}\right)^4 \frac{k^{2-2\epsilon}}{(4\pi)^d}\left[\frac{1}{\epsilon}\left(\frac{1}{72}-\frac{1}{8}\ln 3\right) + O(1)\right]$$
$$+\left(-\frac{\bar\lambda}{1!2!}\right)^4 \frac{k^{-2\epsilon}}{(4\pi)^d}(-i\omega)\left[\frac{1}{\epsilon}\left(\frac{1}{4}-\frac{1}{4}\ln 2\right) + O(1)\right],$$

$$r_5 = r_6 = r_{11} = 0\,.$$

APPENDIX B: INTEGRALS FOR CORRELATION FUNCTIONS

In this Appendix we list all expressions of Feynman graphs of the two-point correlation function and their final results in $2-\epsilon$ dimensions to order $O(1/\epsilon)$.

1. One-loop order

$$
\begin{aligned}
c_0 &= 2D\left(-\frac{\bar\lambda}{1!2!}\right)^2 \int_q \frac{[q\cdot(k-q)]^2}{q^2(k-q)^2q^2+(k-q)^2]} \\
&= 2D\left(-\frac{\bar\lambda}{1!2!}\right)^2 \frac{k^{-\epsilon}}{(4\pi)^{d/2}}\left[\frac{1}{\epsilon}+O(1)\right].
\end{aligned}
$$

2. Two-loop order

$$
\begin{aligned}
c_1 &= 2D\left(-\frac{\bar\lambda}{1!2!}\right)^4 \int_{pq}[q\cdot(k-q)]^2[p\cdot(q-p)]^2 \\
&\quad\times\frac{q^2+p^2+(k-q)^2+(q-p)^2}{q^2p^2(k-q)^2(q-p)^2[q^2+(k-q)^2][q^2+p^2+(q-p)^2]}\frac{1}{p^2+(k-q)^2+(q-p)^2} \\
&= 2D\left(-\frac{\bar\lambda}{1!2!}\right)^4 \frac{k^{-2\epsilon}}{(4\pi)^d}\left[\frac{1}{2}\frac{\Gamma(\epsilon)}{\epsilon}+\frac{1}{\epsilon}\left(\frac{1}{6}-\frac{3}{2}\ln 2+\frac{3}{4}\ln 3\right)+O(1)\right],
\end{aligned}
$$

$$
\begin{aligned}
c_2 &= 2D\left(-\frac{\bar\lambda}{1!2!}\right)^4 \int_{pq}[q\cdot(k-q)]^2[p\cdot(q-p)][-q\cdot(q-p)] \\
&\quad\times\frac{[p^2+(k-q)^2+(q-p)^2][2q^2+(k-q)^2]+2q^4}{q^4(k-q)^2(q-p)^2[q^2+(k-q)^2]^2[q^2+p^2+(q-p)^2]}\frac{1}{p^2+(k-q)^2+(q-p)^2} \\
&= 2D\left(-\frac{\bar\lambda}{1!2!}\right)^4 \frac{k^{-2\epsilon}}{(4\pi)^d}\left[\frac{1}{\epsilon}\left(-\frac{1}{24}-\frac{1}{2}\ln 2+\frac{1}{4}\ln 3\right)+O(1)\right],
\end{aligned}
$$

$$
\begin{aligned}
c_4 &= 2D\left(-\frac{\bar\lambda}{1!2!}\right)^4 \int_{pq}[q\cdot(k-q)][p\cdot(k-p)][(k-p)\cdot(q-p)][q\cdot p] \\
&\quad\times\frac{q^2+p^2+(k-p)^2+(q-p)^2}{q^2p^2(k-p)^2(q-p)^2[q^2+(k-q)^2][q^2+p^2+(q-p)^2]}\frac{1}{[q^2+(k-p)^2+(q-p)^2][p^2+(k-p)^2]} \\
&= 2D\left(-\frac{\bar\lambda}{1!2!}\right)^4 \frac{k^{-2\epsilon}}{(4\pi)^d}\left[-\frac{1}{8}\frac{\Gamma(\epsilon)}{\epsilon}+\frac{1}{\epsilon}\left(-\frac{1}{24}+\frac{1}{8}\ln 2-\frac{1}{16}\ln 3\right)+O(1)\right],
\end{aligned}
$$

$$
\begin{aligned}
c_5 &= 2D\left(-\frac{\bar\lambda}{1!2!}\right)^4 \int_{pq}[q\cdot(k-q)][p\cdot(k-p)][(k-q)\cdot(q-p)][p\cdot(q-p)] \\
&\quad\times\frac{q^2+p^2+2(k-q)^2+(q-p)^2}{p^2(k-q)^2(q-p)^2[q^2+(k-q)^2][q^2+p^2+(q-p)^2]}\frac{1}{[p^2+(k-q)^2+(q-p)^2][p^2+(k-p)^2]} \\
&= 2D\left(-\frac{\bar\lambda}{1!2!}\right)^4 \frac{k^{-2\epsilon}}{(4\pi)^d}\left[\frac{1}{\epsilon}\left(-\frac{1}{12}+\frac{3}{4}\ln 2-\frac{3}{8}\ln 3\right)+O(1)\right],
\end{aligned}
$$

$$
\begin{aligned}
c_6 &= 2D\left(-\frac{\bar\lambda}{1!2!}\right)^4 2\int_{pq}[q\cdot(k-q)][p\cdot(k-p)][(k-p)\cdot(q-p)][-p\cdot(q-p)] \\
&\quad\times\frac{q^2+p^2+(k-p)^2+(q-p)^2}{p^2(k-p)^2(q-p)^2[q^2+(k-q)^2][q^2+p^2+(q-p)^2]}\frac{1}{[q^2+(k-p)^2+(q-p)^2][p^2+(k-p)^2]} \\
&= 2D\left(-\frac{\bar\lambda}{1!2!}\right)^4 \frac{k^{-2\epsilon}}{(4\pi)^d}\left[\frac{1}{4}\frac{\Gamma(\epsilon)}{\epsilon}+\frac{1}{\epsilon}\left(\frac{1}{6}+\frac{3}{4}\ln 2-\frac{3}{8}\ln 3\right)+O(1)\right],
\end{aligned}
$$

$$c_3 = 0\,.$$

APPENDIX C: FLUCTUATION-DISSIPATION THEOREM

In this Appendix we show that the perturbation expansion formalism obeys the fluctuation-dissipation theorem order by order.

1. One-loop order

From the expressions of r_0, c_0, and their corresponding symmetry factors, the one-loop order vertex functions $\Gamma_{11}^{(1)}$ and $\Gamma_{02}^{(1)}$ reduce to

$$\Gamma_{11}^{(1)} = -2 \times 2\nu \left(-\frac{\bar{\lambda}}{1!2!}\right)^2 \int_q \frac{k(k-q)}{q^2+(k-q)^2} ,$$

$$\Gamma_{02}^{(1)} = 2 \times 2D \left(-\frac{\bar{\lambda}}{1!2!}\right)^2 \int_q \frac{1}{q^2+(k-q)^2} .$$

By changing integration variable, we have

$$\int_q \frac{k(k-q)}{q^2+(k-q)^2} = \frac{1}{2} k^2 \int_q \frac{1}{q^2+(k-q)^2} ,$$

which establishes Eq. (19) at the present order.

2. Two-loop order

Similarly, setting $d = 1$, all expressions of r and c reduce to quite simple forms and the vertex functions at this order read

$$\Gamma_{11}^{(2)} = \nu\bar{\lambda}^4 k^2 \int_{pq} \frac{qp[p^2+(k-p)^2]+q(k-p)[q^2+(k-q)^2]}{[q^2+(k-q)^2]^2[p^2+(k-p)^2][p^2+(k-q)^2+(q-p)^2]} ,$$

$$\Gamma_{02}^{(2)} = -2D\bar{\lambda}^4 \int_{pq} \frac{qp[p^2+(k-p)^2]+q(k-p)[q^2+(k-q)^2]}{[q^2+(k-q)^2]^2[p^2+(k-p)^2][p^2+(k-q)^2+(q-p)^2]} ,$$

which imply Eq. (19).

[1] *Surface Disordering: Growth, Roughening and Phase Transitions*, edited by R. Jullien, J. Kertész, P. Meakin, and D. E. Wolf (Nova Science, Commack, NY, 1992).
[2] *Solids Far From Equilibrium*, edited by C. Godréche (Cambridge University Press, Cambridge, England, 1991).
[3] T. Vicsek, *Fractal Growth Phenomena* (World Scientific, Singapore, 1989).
[4] F. Family and T. Vicsek, *Dynamics of Fractal Surfaces* (World Scientific, Singapore, 1991).
[5] F. Family, Physica A **168**, 561 (1990).
[6] M. Plischke and Z. Ràcz, Phys. Rev. Lett. **53**, 415 (1984).
[7] R. Jullien and R. Botet, Phys. Rev. Lett. **54**, 2055 (1985).
[8] F. Family and T. Vicsek, J. Phys. A **18**, L75 (1985).
[9] F. Family, J. Phys. A **19**, L441 (1986).
[10] P. Meakin, P. Ramanlal, L. M. Sander, and R. C. Ball, Phys. Rev. A **34**, 5081 (1986).
[11] D. E. Wolf and J. Kertész, Europhys. Lett. **4**, 651 (1987).
[12] Y. P. Pellegrini and R. Jullien, Phys. Rev. Lett. **64**, 1745 (1990).
[13] J. M. Kim and J. M. Kosterlitz, Phys. Rev. Lett. **62**, 2289 (1989).
[14] M. Kardar, G. Parisi, and Y. C. Zhang, Phys. Rev. Lett. **56**, 889 (1986).
[15] E. Medina, T. Hwa, M. Kardar, and Y. C. Zhang, Phys. Rev. A **39**, 3053 (1989).
[16] D. Forster, D. R. Nelson, and M. J. Stephen, Phys. Rev. A **16**, 732 (1977).
[17] J. Krug, P. Meakin, and T. Halpin-Healy, Phys. Rev. A **45**, 638 (1992).
[18] L. H. Tang, T. Nattermann, and B. M. Forrest, Phys. Rev. Lett. **65**, 2422 (1990).
[19] T. Halpin-Healy, Phys. Rev. Lett. **62**, 442 (1988), Phys. Rev. A **42**, 711 (1990).
[20] T. Nattermann and L. H. Tang, Phys. Rev. A **45**, 7156 (1992).
[21] T. Nattermann and H. Leschhorn, Europhys. Lett. **14**, 603 (1991).
[22] L. H. Tang, B. M. Forrest, and D. E. Wolf, Phys. Rev. A **45**, 7162 (1992).
[23] A. Chakrabarti and R. Toral, Phys. Rev. B **40**, 11 419 (1989).
[24] H. Guo, B. Grossmann, and M. Grant, Phys. Rev. Lett. **64**, 1262 (1990).
[25] B. Grossmann, H. Guo, and M. Grant, Phys. Rev. A **43**, 1727 (1991).
[26] J. Amar and F. Family, Phys. Rev. A **41**, 3399 (1990).
[27] K. Moser, K. Kertész, and D. E. Wolf, Physica A **178**, 215 (1991).
[28] M. Schwartz and S. F. Edwards, Europhys. Lett. **20**, 301 (1992).
[29] J. P. Bouchaud and M. E. Cates, Phys. Rev. E **47**, R1455 (1993); **48**, 635 (1993).
[30] J. Doherty, M. A. Moore, and A. Bray (unpublished).
[31] D. J. Amit, *Field Theory, The Renormalization Group and Critical Phenomena* (McGraw-Hill, New York, 1978).
[32] J. Zinn-Justin, *Quantum Field Theory and Critical Phenomena* (Clarendon Press, Oxford, 1993).
[33] C. De Dominicis and L. Peliti, Phys. Rev. Lett. **38**, 505 (1977); Phys. Rev. B **18**, 353 (1978).
[34] P. C. Martin, E. D. Siggia, and H. A. Rose, Phys. Rev. A **8**, 423 (1973).
[35] R. Bausch, H. K. Janssen, and H. Wagner, Z. Phys. B **24**, 113 (1976).